Research Square

Preprints are preliminary reports that have not undergone peer review.
They should not be considered conclusive, used to inform clinical practice,
or referenced by the media as validated information.

Study on the Mechanism of Acetylcarnitine in Improving Sperm Quality in Busulfan-Induced Azoospermia Mice

Hong Yu
The 970th Hospital of the Joint Logistic Support Force of the Chinese People's Liberation Army
Lipeng Wang
The 968th Hospital of the Joint Logistic Support Force of the Chinese People's Liberation Army ,Jinzhou
Yuexin Yu
Department of Reproductive Medicine, General Hospital of Northern Theater Command
Xiangwei Ma
Department of Reproductive Medicine, General Hospital of Northern Theater Command
Yuhong Xiao
xiaoshugege2@163.com

Department of Reproductive Medicine, General Hospital of Northern Theater Command

Research Article

Keywords: Azoospermia, Acetyl L-carnitine(ALC), Laminin subunit beta 2(LAMB2)

Posted Date: September 27th, 2026

DOI: https://doi.org/10.21203/rs.3.rs-10677370/v1

License: This work is licensed under a Creative Commons Attribution 4.0 International License.
Read Full License

Additional Declarations: No competing interests reported.

Abstract

Background

Azoospermia is a severe form of male infertility. This study examined acetyl L-carnitine (ALC)'s therapeutic effects and molecular mechanisms in busulfan-induced mouse azoospermia.

Methods

Random forest analysis of metabolomics data identified key metabolites in azoospermia patients. Azoospermia was induced in male C57BL/6J mice by intraperitoneal injection of busulfan. Mice were then treated with 0.3% ALC for six consecutive weeks. Sperm concentration, motility, and morphology were assessed. Testicular and epididymal histopathology was evaluated by hematoxylin and eosin staining. ALC levels in testicular tissues were measured by liquid chromatography-tandem mass spectrometry (LC-MS/MS). Transcriptome sequencing was performed to identify differentially expressed genes (DEGs), followed by Gene Ontology (GO) and Kyoto Encyclopedia of Genes and Genomes (KEGG) pathway analyses. Protein expression of laminin subunit beta 2 (LAMB2) was detected by Western blot.

Results

Azoospermia patients exhibited profound acyl-CoA metabolic disturbances. ALC is the critical shuttle for transporting acyl-CoA into mitochondria. ALC treatment significantly restored sperm concentration and motility, reduced sperm malformation rates, and improved testicular and epididymal histopathology in busulfan-induced azoospermic mice. Endogenous ALC levels in the testis were markedly decreased by busulfan and recovered after ALC supplementation. Transcriptomic analysis revealed 35 upregulated and 190 downregulated DEGs in the Busulfan + ALC group compared to the Busulfan group. DEGs enriched in different pathways (e.g., ECM-receptor interaction). ALC reversed the busulfan-induced upregulation of LAMB2.

Conclusion

Acyl-CoA metabolism disorder is a critical metabolic feature in azoospermia. ALC improved busulfan-induced azoospermia in mice, potentially by reversing the upregulation of LAMB2.

Background

Male infertility is a heterogeneous and multifactorial reproductive disorder affecting 7%–12% of the general male population. Azoospermia, defined as the persistent absence of spermatozoa in repeated semen analyses, represents one of the most severe infertility phenotypes and occurs in approximately 1% of men worldwide[1]. In recent years, the prevalence of azoospermia has steadily increased, driven by

deteriorating environmental conditions, widespread unhealthy lifestyles and elevated human exposure to exogenous chemical toxicants[2–4]. Current clinical strategies for azoospermia management primarily include surgical intervention, pharmacological therapy, and assisted reproductive technology(ART)[5–8]. However, these conventional modalities are compromised by inconsistent therapeutic efficacy, low success rates, and substantial financial burdens for patients. Importantly, pharmacological treatments demonstrate marginal therapeutic effects in patients with non-obstructive azoospermia (NOA), which arises from intrinsic spermatogenic dysfunction and constitutes the most clinically intractable subtype of azoospermia[9]. The persistent limitations of existing interventions highlight an urgent clinical need to develop safe, cost-effective, and high- efficacy therapeutic agents to improve the clinical outcomes of azoospermia treatment.

L-carnitine is an endogenous amino acid derivative that serves as an essential regulator of mitochondrial fatty acid β-oxidation and cellular energy homeostasis[10, 11]. By shuttling long-chain fatty acids into mitochondria for oxidative metabolism, L-carnitine sustains energy supply and maintains the physiological stability of reproductive cells. ALC, a biologically active esterified metabolite of L-carnitine[12], exerts crucial protective effects in the male reproductive system via antioxidative, anti-apoptotic, and metabolic regulatory activities[13, 14]. Accumulating clinical evidence has confirmed that ALC supplementation effectively improves sperm motility in patients with oligasthenospermia[15]. Nevertheless, whether ALC can restore impaired spermatogenesis in azoospermia, particularly NOA, remains poorly defined, and the underlying molecular mechanisms have not been systematically elucidated.

In this study, a busulfan-induced azoospermia mouse model was utilized to explore the therapeutic potential of ALC. In vivo experiments were performed to systematically evaluate the effects of ALC supplementation on sperm quality and the structural integrity of testicular and epididymal tissues Furthermore, transcriptome sequencing and comprehensive bioinformatic analyses were performed to identify core target genes and regulatory signaling pathways. This study aims to clarify the therapeutic efficacy and molecular mechanisms of ALC in ameliorating spermatogenic failure, providing novel preclinical evidence for the clinical translation of ALC as a promising NOA therapeutic candidate.

Materials and Methods

Metabolomics Analysis

Male patients visiting the Department of Reproductive Medicine, General Hospital of Northern Theater Command from February to May 2024 were recruited in this study. All research subjects had no metabolic diseases such as diabetes. A total of 85 clinical samples and 10 quality control (QC) samples were included in the metabolomics analysis. In accordance with the criteria specified in the 5th edition of the WHO Laboratory Manual for the Examination and Processing of Human Semen, Samples were divided into five groups: oligospermia group (Group A, N = 20), azoospermia group (Group B, N = 20), asthenospermia group (Group C, N = 10), sperm DNA fragmentation group (Group D, N = 15), and healthy

control group (Group E, N = 20). Diagnostic Criteria for Sperm Abnormalities: (1) Oligozoospermia: It refers to a sperm concentration of less than 15×10^6/mL, or a total sperm count per ejaculate of less than 39×10^6; (2) Azoospermia: It refers to the condition where no sperm are detected under microscopic examination of the sediment after centrifuging semen and post-ejaculatory urine at > 3000g for 15 minutes in three consecutive tests;(3) Asthenospermia: It refers to the condition where the progressive motility of sperm in semen parameters is less than 32% or the total sperm motility is less than 40%; (4) High sperm DNA fragmentation index: It refers to the percentage of sperm with broken DNA strands among all sperm being ≥ 15%.

This study was approved by the Ethics Committee of General Hospital of Northern Theater Command (Ethics Review No. ER 2023(6), approval date: 12/12/2023). All participants provided written informed consent, and the research was performed in accordance with the Declaration of Helsinki.

Each 100 μL sample was mixed with 400 μL methanol–acetonitrile (1:1, v/v) spiked with isotope-labeled internal standards. The mixture was vortexed for 30 s, sonicated in an ice-water bath for 10 min, incubated at -40°C for 1 h, and centrifuged at 12,000 rpm (13,800 ×g, radius 8.6 cm) at 4°C for 15 min. The supernatant was collected and transferred into an injection vial for instrumental analysis. An equal volume of supernatant from all samples was mixed to prepare QC samples. Metabolite separation was performed on a Vanquish ultra-high-performance liquid chromatography (UHPLC) system (Thermo Fisher Scientific Inc., Waltham, USA) coupled with an Orbitrap Exploris 120 high-resolution mass spectrometer (Thermo Fisher Scientific Inc.). Chromatographic separation was carried out using a Waters ACQUITY UPLC BEH Amide column (2.1 mm × 50 mm, 1.7 μm). Mobile phase A was water containing 25 mmol/L ammonium acetate and 25 mmol/L ammonia water, and mobile phase B was acetonitrile. The sample tray temperature was maintained at 4 ℃, and the injection volume was 2 μL. Xcalibur software was used for mass spectrometry data acquisition with the following parameters: sheath gas flow rate, 50 arbitrary unit (Arb); auxiliary gas flow rate, 15 Arb; capillary temperature, 320°C; full mass spectrometry (MS) resolution, 60,000; tandem mass spectrometry (MS/MS) resolution, 15,000; normalized collision energy (NCE), 20/30/40; spray voltage, 3.8 kilovolt (Kv) in positive mode and − 3.4 kV in negative mode. Data were processed using outlier filtering based on relative standard deviation (RSD), missing-value filtering, half-minimum imputation, and internal-standard normalization. Only peaks with missing values ≤ 50% across all groups were retained during filtering, and 36,356 peaks were ultimately used for subsequent analysis.

Screening of Key Metabolites

Key metabolites between the azoospermia and control groups were screened using the random forest (RF) algorithm with the randomForest package in R, and metabolites with a q-value < 0.05 were included. During the analysis, the ntree parameter was evaluated from 1 to 500 to identify the optimal value that minimized the model's out-of-bag (OOB) error. Then, based on the optimized ntree value, the RF model was constructed to compare and rank the mean decrease accuracy (MDA) values of the metabolites, and the top 10 metabolites were finally identified. Receiver operating characteristic (ROC) curve analysis

was conducted using the pROC package to evaluate the diagnostic performance of the top 10 metabolites, and the area under the curve (AUC) was calculated for each metabolite. The Wilcoxon rank-sum test was used to verify the differential abundance of the top 10 metabolites between the azoospermia and control groups.

Animals and Experimental Design

Male C57BL/6J mice (8–10 weeks old, weighing 26–28 g) were purchased from the SPF Biotechnology Co., Ltd (Beijing, China). All mice were housed under a natural light-dark rhythm, with standard temperature and humidity conditions. Animals could obtain sufficient feed and drinking water ad libitum during the experiment period. After one week of adaptive feeding, all mice were randomly assigned to the Control group, Busulfan (Meryer Biochemical Technology Co., Ltd, Shanghai, China) group, and Busulfan + ALC (Aladdin Biochemical Technology Co., Ltd, Shanghai, China) group ($N \geq 6$). To establish a mouse azoospermia model, busulfan was administered intraperitoneally. The control mice were injected with normal saline, while mice in the Busulfan and Busulfan + ALC groups received two 20 mg/kg busulfan injections at a 3-hour interval (total dose: 40 mg/kg)[16, 15]. Following the establishment of the azoospermia model, mice in the Control and Busulfan groups received normal drinking water, whereas those in the Busulfan + ALC group were treated with 0.3% ALC in their drinking water daily for six consecutive weeks. This concentration and route of administration of ALC have been previously shown to be effective and well-tolerated in mice[17]. After treatment completion, all mice were euthanized via inhalation anesthesia with 5% isoflurane, and the testes and epididymides were rapidly removed. Then, one testis together with its epididymis from each mouse was fixed for histopathological analysis, while the other testis was snap-frozen in liquid nitrogen and stored at − 80°C for subsequent analyses. Additionally, epididymal spermatozoa were collected from the cauda epididymidis. The Animal Medical Research Ethics Subcommittee of the General Hospital of Northern Theater Command approved all animal experiments described herein (Approval No. 2025 − 135). Throughout the study, all animal handling, breeding, and experimental procedures were strictly implemented in accordance with national guidelines for laboratory animal care and ethical principles, with the well-being and ethical entitlements of the animals rigorously protected, and maximum efforts undertaken to minimize their suffering and discomfort.

Sperm Motility, Concentration, and Morphology Assessment

Spermatozoa were collected from the freshly excised cauda epididymidis and incubated in phosphate-buffered saline (PBS) at 37°C for 10 minutes to allow sperm to swim out. The sperm suspension was loaded onto a Neubauer counting chamber covered with a coverslip and examined under a microscope (Olympus Corporation, Tokyo, Japan). Sperm motility and concentration were evaluated by counting each sample three times and calculating the average, with motility expressed as the percentage of progressively motile sperm. An aliquot of 10–20 μL of the sperm suspension was dropped onto one end of a clean glass slide, and a thin smear was prepared by spreading the drop at an angle of approximately

30° to the slide surface using a second clean slide. The smear was air-dried at room temperature, fixed in methanol for 5–10 minutes, and then again air-dried. Sperm morphology was observed under a microscope.

Giemsa Staining

Giemsa working solution (1×, Beyotime Biotechnology, Shanghai, China) was prepared according to the manufacturer's instructions. The fixed sperm smears were stained with Giemsa working solution for 45 minutes, gently rinsed with distilled water, air-dried, and then observed and photographed under a microscope. At least 150 spermatozoa per mouse were counted. The sperm malformation rate (%) was calculated as (number of malformed sperm / total sperm counted) × 100%.

Liquid Chromatography-Tandem Mass Spectrometry (LC-MS/MS)

Frozen mouse testicular tissues were thawed, rinsed thoroughly with pre-cooled PBS, and minced. The tissue was thoroughly homogenized in an ice-water bath using pre-cooled methanol. The homogenate was centrifuged at 12,000 × g for 15 minutes at 4°C, and the supernatant was collected for analysis. A series of ALC standard solutions (10 – 1,000 ng/mL) was prepared in methanol and filtered through a 0.22 μm filter. The concentration of ALC in supernatant was determined using the LC-MS/MS system and calculated based on the standard curve.

Hematoxylin and Eosin (HE) Staining

Mouse testes and epididymides were fixed in paraformaldehyde (Beyotime Biotechnology). Fixed tissues were dehydrated in graded ethanol solutions, cleared in xylene, embedded in paraffin, and sectioned at 4 μm paraffin blocks. The sections were deparaffinized and rehydrated, then stained with hematoxylin (Servicebio Technology Co., Ltd., Wuhan, China) and alcoholic eosin (Servicebio Technology Co., Ltd.). After subsequent dehydration and transparency, the sections were mounted with neutral balsam. Stained specimens were observed under the microscope.

Transcriptome Sequencing

Total RNA was isolated from testicular tissues of the Busulfan and Busulfan + ALC groups using TRIzol Reagent (Thermo Fisher Scientific Inc.). The mRNA was enriched using oligo (dT)-coated magnetic beads and randomly fragmented (94°C for 5–15 minutes, fragment length 300–400 bp). First-strand cDNA was synthesized using random hexamer primers and reverse transcriptase, followed by second-strand cDNA synthesis with deoxyuridine triphosphate (dUTP)-containing deoxyribonucleoside triphosphates (dNTPs) for strand-specific labeling. Double-stranded cDNA underwent end repair, A-tailing, and adapter ligation. Subsequent PCR amplification and magnetic bead purification were

conducted to construct strand-specific libraries, which were then sequenced on the Illumina platform (Illumina, Inc., San Diego, CA, USA). Raw data were processed to remove adapters and low-quality reads, yielding clean data for subsequent analysis. Differentially expressed genes (DEGs) between the Busulfan and Busulfan + ALC groups were identified using the DESeq2 package in R. The false discovery rate (FDR) was controlled using the Benjamini-Hochberg procedure. Genes with an absolute $\log_2$ fold change ($|\log_2 FC|$) ≥ 0.26 were considered statistically significant DEGs. Finally, the Gene Ontology (GO) and Kyoto Encyclopedia of Genes and Genomes (KEGG) databases were used to further explore the biological functions and signaling pathways of the DEGs.

Western Blot (WB)

Total protein from testis tissue was extracted using radioimmunoprecipitation assay (RIPA) lysis buffer (Servicebio Technology Co., Ltd.), and the protein concentration was measured using a Pierce bicinchoninic acid (BCA) Protein Assay Kit (Thermo Fisher Scientific Inc.). A total of 20 μg of protein per well was separated by sodium dodecyl sulfate-polyacrylamide gel electrophoresis (SDS-PAGE) and transferred onto polyvinylidene fluoride (PVDF) membranes (Millipore, Billerica, USA). The membranes were blocked with 5% non-fat milk, then incubated overnight at 4°C with primary antibodies against LAMB2(Cat. No. ab277521, Abcam, Cambridge, UK) and beta-actin (Cat. No. ab8227, Abcam) at a dilution of 1:1000. After washing with Tris-buffered saline with Tween-20 (TBST), the membranes were incubated with HRP-conjugated secondary antibodies (Cat. No. ab6721, Abcam) at a dilution of 1:5000 for 1 hour at room temperature. Protein bands were visualized with enhanced chemiluminescence (ECL) reagent using a chemiluminescence imaging system (Tanon Science & Technology Co., Ltd., Shanghai, China), and images were acquired. Quantitative analysis was conducted via ImageJ software.

Statistical Analysis

All statistical analyses were performed using R software (version 4.5.2), GraphPad Prism 8.0, and SPSS 20.0. Data were expressed as mean ± standard deviation (SD). For metabolomics data, ROC analysis was applied to evaluate the diagnostic performance of the top 10 metabolites, and the Wilcoxon rank-sum test was used to assess their differential abundance between azoospermia patients and controls. For transcriptomic data, DEGs with FDR < 0.05 and |log2FC| ≥ 0.26 were considered statistically significant. Comparisons among multiple groups were made using one-way ANOVA followed by Tukey's multiple comparisons test. A p-value < 0.05 was considered statistically significant unless otherwise specified.

Results

Screening and Validation of Key Diagnostic Metabolites for Azoospermia

A total of 1,315 metabolites with a q-value < 0.05 were subjected to RF analysis to identify key metabolites between the azoospermia and control groups. The OOB error was rapidly reduced within the

first 20 decision trees, gradually stabilized after 100 trees, and remained at a low level without obvious overfitting, indicating that 100 trees were selected as the optimal number of trees (Supplementary Fig. 1). The top 10 metabolites were Citicoline, Compound WIN VIII, trans-2-[(Dimethylamino)methylimino]-5-[2-(5-nitro-2-furyl)-vinyl]-1,3,4-oxadiazole, Octanoyl-CoA, Acetoacetyl-CoA, trans-Oct-2-enoyl-CoA, Myricetin 3-arabinoside, QYNAD, dTDP-3-amino-2,3,6-trideoxy-4-keto-D-glucose, and Malonyl-CoA (Fig. 1). ROC curve analysis revealed that all top 10 metabolites achieved AUC values greater than 0.9, suggesting favorable diagnostic performance for azoospermia (Fig. 2). Wilcoxon rank-sum test further showed that compared with the control group, the azoospermia group had significantly lower levels of citicoline, Compound WIN VIII, octanoyl-CoA, acetoacetyl-CoA, trans-oct-2-enoyl-CoA, myricetin 3-arabinoside, QYNAD, and malonyl-CoA. By contrast, trans-2-[(dimethylamino)methylimino]-5-[2-(5-nitro-2-furyl)-vinyl]-1,3,4-oxadiazole and dTDP-3-amino-2,3,6-trideoxy-4-keto-D-glucose were markedly elevated in the azoospermia group (Fig. 3). In line with previous reports, acyl-CoAs have been directly implicated in the steps of fatty acid β-oxidation (FAO)[18]. Specifically, octanoyl-CoA and trans-oct-2-enoyl-CoA are key intermediates in the mitochondrial β-oxidation spiral[19]; acetoacetyl-CoA is a normal intermediate generated during fatty acid breakdown[20]; and malonyl-CoA functions as a critical regulator, allosterically inhibiting carnitine palmitoyltransferase 1 (CPT-1) to control the rate of fatty acid entry into mitochondria[21]. These findings indicated that acyl-CoA metabolism was dysregulated in azoospermia. Although ALC was not among the top 10 differential metabolites, it serves as a key carrier for transporting acyl-CoAs into mitochondria and is essential for maintaining acyl-CoA homeostasis[22]. Given the significant perturbation of this metabolic pathway and the central role of ALC in its regulation, ALC was selected as a candidate for subsequent experimental verification.

ALC Ameliorated Busulfan-Induced Azoospermia in Mice

Microscopic observation of sperm morphology revealed that sperm in the Control group exhibited a typical tadpole shape with clear head contours and complete long tails. In the Busulfan group, sperm count was drastically reduced, and most sperm showed head malformation, tail curling, or absence. In the Busulfan + ALC group, sperm morphology was markedly improved, accompanied by decreased abnormal spermatozoa, and its morphology was close to that of the Control group (Fig. 4A).Sperm concentration and motility were significantly decreased in the Busulfan group compared with the Control group, and oral administration of ALC significantly restored sperm concentration and motility (Fig. 4B-C). Giemsa staining revealed frequent sperm malformations, including abnormal head morphology and tail fracture in the Busulfan group, and these defects were obviously alleviated in the Busulfan + ALC group (Fig. 4D). Statistical analysis of sperm malformation rates confirmed that busulfan triggered sperm malformation, whereas ALC treatment alleviated busulfan-induced sperm damage (Fig. 4E). Chromatographic analysis showed that the endogenous ALC level in the testis was markedly decreased in the busulfan group and recovered significantly after exogenous ALC supplementation (Fig. 4F). HE staining demonstrated that the seminiferous tubules contained multiple layers of spermatogenic cells and numerous mature sperm in the Control group, and the epididymal lumen was filled with sperm. In the

Busulfan group, seminiferous tubules were atrophied, spermatogenic cells were disorganized, and sperm were rarely observed in the tubular lumen. In the Busulfan + ALC group, the thickness of the seminiferous epithelium was increased, the number of spermatogenic cells at all levels was elevated, and the sperm count in the epididymis was significantly recovered (Fig. 4G-H). These results indicated that ALC effectively alleviated busulfan-induced spermatogenic dysfunction, improved sperm count, motility, and morphology, and mitigated pathological damage to testicular and epididymal tissues.

Mechanistic Analysis of ALC Amelioration of Azoospermia

Transcriptome sequencing was performed on testis tissue from the model and acetylcarnitine-treated groups. A large number of DEGs were screened out, comprising 35 upregulated and 190 downregulated genes in the Busulfan + ALC group compared to the Busulfan group. A volcano plot visualized these changes (Fig. 5A). Cluster heatmap analysis further revealed distinct gene expression patterns between the two groups (Fig. 5B). GO enrichment analysis revealed that DEGs were significantly enriched in multiple GO terms. For biological processes (BPs), the enriched terms mainly included biological adhesion, regulation of cell motility, cell adhesion, regulation of cellular component movement, and gland morphogenesis. In terms of cellular components (CCs), the top-enriched categories were the extracellular region, vesicle, extracellular space, extracellular region part, and extracellular exosome. Regarding molecular functions (MFs), transmembrane receptor protein kinase activity was prominently enriched (Fig. 5C, all p-values < 0.000001). KEGG enrichment analysis demonstrated that DEGs were markedly enriched in the phosphatidylinositol 3-kinase-protein kinase B (PI3K-Akt) signaling pathway, focal adhesion, amoebiasis, glycolysis/gluconeogenesis, and extracellular matrix (ECM)-receptor interaction pathways (Fig. 5D, all p-values < 0.001). The PPI network was constructed based on DEGs via the Retrieval of Interacting Genes/Proteins (STRING) database, which revealed complex interactions among DEGs (Fig. 6). Subsequently, DEGs were imported into the Cytoscape software to identify the core gene. The highest-scoring gene in the PPI network contained laminin subunit alpha 4 (LAMA4), laminin subunit gamma 1 (LAMC1), laminin subunit alpha 1 (LAMA1), laminin subunit gamma 3 (LAMC3), integrin subunit alpha 9 (ITGA9), and LAMB2 (Fig. 7A). Except for ITGA9, all other genes were laminin subunits. According to previous studies, thickened testicular basement membrane and markedly elevated laminin expression were observed in patients with oligospermia and asthenospermia, among which LAMB2 presented the most significant upregulation, suggesting that LAMB2 might serve as a crucial target for azoospermia[23]. WB was therefore applied to detect LAMB2 protein expression. The results showed that the LAMB2 protein level was significantly increased in testicular tissues of the Busulfan group compared with the Control group, and this upregulation was distinctly reversed after ALC treatment (Fig. 7B).

Discussion

Patients with azoospermia display prominent lipid metabolic disturbances, and acyl-CoA metabolic imbalance represents a vital metabolic signature of azoospermia. In the present study, we systematically

evaluated the therapeutic effect of ALC using a busulfan-induced murine azoospermia model. The results revealed that ALC ameliorates busulfan-induced spermatogenic failure in mice.

Fatty acid β-oxidation serves as the primary energy source for sperm maturation and motility. Sertoli cells (SCs) within the testicular microenvironment also provide indirect metabolic and structural support to spermatogenic cells via fatty acid β-oxidation[24]. Prior human cohort studies have broadly correlated dysregulated lipid profiles with male infertility, but few investigations have pinpointed a panel of specific acyl-CoA intermediates as diagnostic and pathogenic biomarkers for azoospermia. In this study,random forest (RF) analysis demonstrated that the levels of Octanoyl-CoA, Acetoacetyl-CoA, Malonyl-CoA and trans-Oct-2-enoyl-CoA were significantly reduced in patients with azoospermia. ALL four metabolites belong to the acyl-CoA family and are involved in fatty acid β-oxidation. These four metabolites collectively constitute key nodes within the fatty acid β-oxidation pathway: octanoyl-CoA acts as a central intermediate mediating mitochondrial fatty acid uptake and catabolism[25, 26]; acetoacetyl-CoA represents the terminal catalytic product of each β-oxidation cycle[27]; malonyl-CoA functions as a canonical negative regulator governing the rate of mitochondrial β-oxidation flux[28]; and trans-oct-2-enoyl-CoA participates in sequential dehydrogenation reactions during acyl chain breakdown[29].Concomitant downregulation of these four functionally interconnected acyl-CoA species cannot be interpreted as isolated metabolic fluctuations; instead, this coordinated depletion indicates a global suppression of testicular fatty acid catabolism. Mechanistically, compromised β-oxidation ablates the primary energy pool required for germ cell proliferation, differentiation, and post-meiotic sperm maturation, while simultaneously disrupting the paracrine metabolic support supplied by SCs to the seminiferous epithelium. These observations advance the current literature by refining the vague association between lipid dysregulation and azoospermia to a concrete pathogenic axis centered on impaired acyl-CoA-dependent β-oxidation.

The results demonstrated that supplementation with ALC significantly restored sperm count, progressive motility, and normal sperm morphology, alleviated structural damage to seminiferous tubules and epididymal tissue, and reversed the metabolic collapse of acyl-CoA pools in azoospermic mice. Carnitine and its acetylated derivative ALC are well-established lipid transporters that modulate the intramitochondrial acetyl-CoA/CoA ratio to mitigate mitochondrial lipotoxicity and oxidative damage to germ cells[30].Meanwhile, they nourish SCs and are critical for sperm maturation and motility acquisition[31, 32]. The male reproductive tract, particularly the epididymis, accumulates extraordinarily high physiological concentrations of carnitine to support sperm capacitation and motility acquisition[33], and ALC is the most abundant and widely distributed acyl-carnitine isoform in mammalian testicular tissue[34]. Previous clinical reports have only documented the empirical fertility-improving effects of carnitine analogs. The present study further elucidated the core mechanism of action and proposed a hypothesis of dual regulatory patterns exerted by intratesticular ALC: first, ALC shuttles excess toxic acyl-CoA moieties out of the mitochondrial matrix to rebalance the acyl-CoA pool and recover suppressed fatty acid β-oxidation, thereby replenishing energy substrates for germ cell development; Second, ALC may provide trophic support for SCs and preserve their metabolic functions, thus reconstructing a suitable seminiferous tubular microenvironment and indirectly facilitating the

progression of spermatogenesis. Direct experimental evidence clarifying whether acetyl-L-carnitine (ALC) intervention restores the core acyl-CoA metabolic network in toxicant-induced azoospermia models remains lacking. This mechanistic model fills this important research gap and verifies that the therapeutic efficacy of ALC is associated with normalization of disturbed acyl-CoA and β-oxidation pathways. Multiple clinical trials support this hypothesized mechanism, revealing that combined supplementation of L-carnitine, α-lipoic acid, trace elements and antioxidants ameliorates semen parameters in patients with oligoasthenozoospermia[35, 23, 36, 37], consistent with the results of this in vivo preclinical investigation.Collectively, our findings establish ALC as a targeted metabolic modulator rather than a non-specific antioxidant, providing a mechanistic basis for expanding ALC clinical application to patients with azoospermia driven by lipid metabolic defects.

Transcriptomic and bioinformatic analyses revealed that the expression of LAMB2 protein was significantly upregulated in testicular tissues of azoospermic mice compared with control groups, suggesting that LAMB2 may serve as a key target underlying azoospermia. LAMB2 constitutes the primary building block of the testicular basement membrane[38, 39]. it orchestrates basement membrane assembly and regulates fundamental cellular processes including adhesion, differentiation, and paracrine signal transduction within the seminiferous epithelium[40]. pathological overexpression of LAMB2 promotes excessive ECM deposition and basement membrane thickening. The intact basement membrane is essential for maintaining SCs polarity, germ cell attachment, and intercellular metabolic communication between somatic and germ cell populations [41, 42]; thickened basement membranes physically and biochemically impede nutrient and metabolite transport across the seminiferous barrier, ultimately arresting spermatogenic differentiation. Consistent with our murine data, clinical transcriptomic cohorts have documented elevated LAMB2 expression in patients with oligozoospermia and asthenozoospermia, implying a conserved pathogenic role across human and murine spermatogenic disorders[23]. Notably, multi-omics integration further positioned LAMB2 as a downstream effector modulated by ALC intervention. This work proposed a previously unreported regulatory axis: ALC-mediated restoration of fatty acid metabolism suppresses aberrant LAMB2 transcription, attenuates pathological basement membrane remodeling, and rescues disrupted spermatogenesis Prior reproductive research has separately investigated either testicular metabolic dysfunction or ECM remodeling in male infertility, yet no prior work has integrated these two independent pathogenic pathways to construct a unified therapeutic regulatory network centered on ALC and LAMB2. we bridged lipid metabolic homeostasis and ECM structural integrity to delineate a complete pathogenic cascade for toxicant-induced azoospermia, and identified LAMB2 as a druggable molecular target linking metabolic correction to testicular microenvironment repair.

In this study, transcriptomic profiling and bioinformatic analyses were primarily utilized to predict the functional pathways and molecular targets of ALC. Nevertheless, several limitations remain regarding methodology and experimental validation.First, all therapeutic efficacy assessments based on a single fixed ALC dosage in mice, precluding quantitative analysis of dose-response relationships. Future in vivo experimentation should establish a gradient of ALC dosages to quantify the dose-response relationship between ALC concentration and three key indicators: acyl-CoA metabolic recovery, LAMB2 expression

levels, and semen phenotypic recoverySecond, the regulatory interaction between ALC, fatty acid β-oxidation signaling, and LAMB2 was predicted solely via transcriptomic and bioinformatic analyses without direct genetic or pharmacological verification. Follow-up mechanistic experiments are warranted to dissect whether LAMB2 upregulation is a necessary and sufficient driver of basement membrane thickening and spermatogenic arrest.

In summary, the present work established acyl-CoA metabolic suppression and LAMB2-mediated basement membrane remodeling as core pathogenic mechanisms of busulfan-induced azoospermia, and supported ALC as a multi-target therapeutic agent capable of restoring both testicular metabolic homeostasis and ECM structural integrity. The integrated metabolomic-transcriptomic framework established herein offers a template to dissect complex metabolic-microenvironmental crosstalk in male reproductive disorders. Meanwhile, the acyl-CoA biomarker signature and LAMB2 molecular target deliver tangible translational resources for future diagnostic and therapeutic development against azoospermia.

Declarations

Ethics approval and consent to participate:

The experiments conformed to the Guide for the Care and Use of Laboratory Animals. Animal study has been approved by the Animal Ethics Committee of the General Hospital of Northern Theater Command (Approval No. 2025-135).

All methods are reported in accordance with ARRIVE guidelines.

Consent for publication:

Not applicable.

Availability of data and materials:

The datasets generated and/or analysed during the current study are available in the BioProject repository, https://dataview.ncbi.nlm.nih.gov/object/PRJNA1520802?reviewer=vdusem4gotp4tcmdalv7il8omb.

Competing interests:

The author declares that he have no competing interests.

Funding:

This work was supported by the Science and Technology Joint Program of Liaoning Province (Grant No. 2024JH2/102600271).

Author contributions:

Yuhong Xiao,Hong Yu and Lipeng Wang conceived and designed the study. Yuhong Xiao and Xiangwei Ma performed the experiments and prepared the figures and tables. Yuexin Yu performed the bioinformatics analysis. Hong Yu and Lipeng Wang drafted the manuscript. Yuhong Xiao revised it critically for important intellectual content. All authors have read and approved the manuscript.

Acknowledgements:

Not applicable.

Clinical trial number:

Not applicable.

References

1. Cioppi F, Rosta V, Krausz C. Genetics of Azoospermia. Int J Mol Sci. 2021;22(6). 10.3390/ijms22063264.
2. Margiana R, Odhar HA, Prasad KDV, Oghenemaro EF, Kumawat MMR, Uthirapathy R, Sharma S, Kumar S, Nouri MR M. Does outdoor air pollution cause poor semen quality? A systematic review and meta-analysis. BMC Urol. 2025;25(1). 10.1186/s12894-025-01728-4.
3. Szabó A, Nyirády P, Kopa Z. Impact of lifestyle and environmental factors on fertility. Curr Opin Urol. 2025;35(6):685–90. 10.1097/mou.0000000000001339.
4. Alhamam A, Garabed LR, Julian S, Flannigan R. The association of medications and supplements with human male reproductive health: a systematic review. Fertil Steril. 2023;120(6):1112–37. 10.1016/j.fertnstert.2023.10.021.
5. Rambhatla A, Kavoussi PK, Shah R, Agarwal A. Management of non-obstructive azoospermia: advances, challenges, and expert recommendations. Asian J Androl. 2025;27(3):277–8. 10.4103/aja202539.
6. Jensen CFS, Ohl DA, Fode M, Jørgensen N, Giwercman A, Bruun NH, Elenkov A, Klajnbard A, Andersen CY, Aksglaede L, Grøndahl ML, Bekker MC, Sønksen J. Microdissection Testicular Sperm Extraction Versus Multiple Needle-pass Percutaneous Testicular Sperm Aspiration in Men with Nonobstructive Azoospermia: A Randomized Clinical Trial. Eur Urol. 2022;82(4):377–84. 10.1016/j.eururo.2022.04.030.
7. Tharakan T, Corona G, Foran D, Salonia A, Sofikitis N, Giwercman A, Krausz C, Yap T, Jayasena CN, Minhas S. Does hormonal therapy improve sperm retrieval rates in men with non-obstructive azoospermia: a systematic review and meta-analysis. Hum Reprod Update. 2022;28(5):609–28. 10.1093/humupd/dmac016.
8. Tharakan T, Luo R, Foran D, Smith M, Jayasena CN, Minhas S. Strategies in Infertile Azoospermic Patients with Negative Microdissection Testicular Sperm Extraction Surgery. Urol Res Pract.

2023;49(2):65–72. 10.5152/tud.2020.20435.

9. Alriyalat S, Deameh MG, Farraj H, Alsmadi JK, Bani Irshid BA, Abu Rahmeh H, Awawdeh AK, Mubarak MA, Ababneh AF, Bani Amer WeA, Al-Zubi M. (2025) Predictors of sperm retrieval success in first-time and repeated Micro-TESE for nonobstructive azoospermia. Future Science OA 11 (1). 10.1080/20565623.2025.2511449
10. Adeva-Andany MM, Carneiro-Freire N, Seco-Filgueira M, Fernández-Fernández C, Mouriño-Bayolo D. Mitochondrial β-oxidation of saturated fatty acids in humans. Mitochondrion. 2019;46:73–90. 10.1016/j.mito.2018.02.009.
11. Sisi M, Yong L, Lixing Q, Changsheng G, Jin Y, Hang Z, Xing C, Heng L. L-carnitine: new perspectives on the management of preterm infants. Front Nutr. 2025;12:1508441. 10.3389/fnut.2025.1508441.
12. Ferreira GC, McKenna MC. l-Carnitine and Acetyl-l-carnitine Roles and Neuroprotection in Developing Brain. Neurochem Res. 2017;42(6):1661–75. 10.1007/s11064-017-2288-7.
13. Qiao N, Chen H, Du P, Kang Z, Pang C, Liu B, Zeng Q, Pan J, Zhang H, Mehmood K, Tang Z, Li Y, Ortega A. (2021) Acetyl-L-Carnitine Induces Autophagy to Promote Mouse Spermatogonia Cell Recovery after Heat Stress Damage. BioMed Research International 2021 (1). 10.1155/2021/8871328
14. Zou YJ, Yang J, Chang S, Xu WM, Yin TL, Long W. Acetyl-L-carnitine: An effective antioxidant against cryo-damage on human spermatozoa with asthenospermia. J Huazhong Univ Sci Technolog Med Sci. 2017;37(6):915–21. 10.1007/s11596-017-1827-4.
15. Zhang X, Cui Y, Dong L, Sun M, Zhang Y. The efficacy of combined l-carnitine and l-acetyl carnitine in men with idiopathic oligoasthenoteratozoospermia: A systematic review and meta-analysis. Andrologia. 2020;52(2):e13470. 10.1111/and.13470.
16. Kim KH, Park MJ, Park NC, Park HJ. Effect of N-acetyl-L-cysteine on Testicular Tissue in Busulfan-Induced Dysfunction in the Male Reproductive System. world J men's health. 2023;41(4):882–91. 10.5534/wjmh.220100.
17. Cherix A, Larrieu T, Grosse J, Rodrigues J, McEwen B, Nasca C, Gruetter R, Sandi C. Metabolic signature in nucleus accumbens for anti-depressant-like effects of acetyl-L-carnitine. eLife. 2020;9. 10.7554/eLife.50631.
18. Szrok-Jurga S, Czumaj A, Turyn J, Hebanowska A, Swierczynski J, Sledzinski T, Stelmanska E. The Physiological and Pathological Role of Acyl-CoA Oxidation. Int J Mol Sci. 2023;24(19). 10.3390/ijms241914857.
19. Kelly DP, Whelan AJ, Ogden ML, Alpers R, Zhang ZF, Bellus G, Gregersen N, Dorland L, Strauss AW. Molecular characterization of inherited medium-chain acyl-CoA dehydrogenase deficiency. Proc Natl Acad Sci USA. 1990;87(23):9236–40. 10.1073/pnas.87.23.9236.
20. Ding X, Wu J, Wang L, Li K, Gao H, Wu M, Zhang Q, Han R, Wang W, Xiao W. β–hydroxybutyric acid as a potential therapeutic metabolite for type 2 diabetes mellitus (Review). Int J Mol Med. 2026;57(1). 10.3892/ijmm.2025.5683.

21. Ruderman NB, Saha AK, Vavvas D, Witters LA. Malonyl-CoA, fuel sensing, and insulin resistance. Am J Physiol. 1999;276(1):E1–18. 10.1152/ajpendo.1999.276.1.E1.
22. Zhang YM, Chohnan S, Virga KG, Stevens RD, Ilkayeva OR, Wenner BR, Bain JR, Newgard CB, Lee RE, Rock CO, Jackowski S. Chemical knockout of pantothenate kinase reveals the metabolic and genetic program responsible for hepatic coenzyme A homeostasis. Chem Biol. 2007;14(3):291–302. 10.1016/j.chembiol.2007.01.013.
23. Ooba T, Ishikawa T, Yamaguchi K, Kondo Y, Sakamoto Y, Fujisawa M. Expression and distribution of laminin chains in the testis for patients with azoospermia. J Androl. 2008;29(2):147–52. 10.2164/jandrol.107.003210.
24. Fukasawa M, Atsuzawa K, Mizutani K, Nakazawa A, Usuda N. Immunohistochemical Localization of Mitochondrial Fatty Acid β-Oxidation Enzymes in Rat Testis. J Histochem Cytochemistry. 2009;58(2):195–206. 10.1369/jhc.2009.954693.
25. Nada MA, Rhead WJ, Sprecher H, Schulz H, Roe CR. Evidence for Intermediate Channeling in Mitochondrial β -Oxidation. J Biol Chem. 1995;270(2):530–5. 10.1074/jbc.270.2.530.
26. Hashimoto F, Furuya Y, Hayashi H. Accumulation of medium chain acyl-CoAs during beta-oxidation of long chain fatty acid by isolated peroxisomes from rat liver. Biol Pharm Bull. 2001;24(6):600–6. 10.1248/bpb.24.600.
27. Kotkina TI, Titov VN, Parkhimovich RM. (2014) [The different notions about beta-oxidation of fatty acids in peroxisomes, peroxisomes and ketonic bodies. The diabetic, acidotic coma as an acute deficiency of acetyl-CoA and ATP]. Klin Lab Diagn (3):14–23.
28. Paulson DJ, Ward KM, Shug AL. Malonyl CoA inhibition of carnitine palmityltransferase in rat heart mitochondria. FEBS Lett. 1984;176(2):381–4. 10.1016/0014-5793(84)81201-6.
29. Hiltunen JK, Qin Y. beta-oxidation - strategies for the metabolism of a wide variety of acyl-CoA esters. Biochim Biophys Acta. 2000;1484(2–3):117–28. 10.1016/s1388-1981(00)00013-5.
30. Leitão AMF, Silva BR, Barbalho EC, Paulino LRM, Costa FDC, Martins FS, Silva JRV. The role of L-carnitine in the control of oxidative stress and lipid β-oxidation during in vitro follicle growth, oocyte maturation, embryonic development and cryopreservation: a review. Zygote. 2024;32(5):335–40. 10.1017/s096719942400039x.
31. Shah W, Khan R, Shah B, Khan A, Dil S, Liu W, Wen J, Jiang X. The Molecular Mechanism of Sex Hormones on Sertoli Cell Development and Proliferation. Front Endocrinol. 2021;12. 10.3389/fendo.2021.648141.
32. Li D, Jiang N, Pan M, Ma L, Huang Y, Xu X, Yang X, Zhu Y, Shi H, Zhao SC. OCTN2 expression and function in the Sertoli cells of testes from patients with non-obstructive azoospermia. J Mol Histol. 2024;56(1):31. 10.1007/s10735-024-10298-y.
33. Ng CM, Blackman MR, Wang C, Swerdloff RS. The Role of Carnitine in the Male Reproductive System. Ann N Y Acad Sci. 2009;1033(1):177–88. 10.1196/annals.1320.017.
34. Brass EP, Hoppel CL. Relationship between acid-soluble carnitine and coenzyme A pools in vivo. Biochem J. 1980;190(3):495–504. 10.1042/bj1900495.

35. Golan R, Weissenberg R, Lewin LM. Carnitine and acetylcarnitine in motile and immotile human spermatozoa. Int J Androl. 1984;7(6):484–94. 10.1111/j.1365-2605.1984.tb00805.x.
36. Ioannidou P, Zeginiadou T, Venetis C, Papanikolaou D, Zepiridis L, Savvaidou D, Chatzimeletiou K, Lambropoulos A, Goulis DG, Grimbizis G, Kolibianakis EM. The Effect of Antioxidant Administration on Semen Quality in Men with Infertility: A Randomized Placebo-Controlled Clinical Trial. Antioxid (Basel). 2025;14(4). 10.3390/antiox14040488.
37. Sun X, Zhang L, Kang Y, Wang X, Jiang C, Wang J, Sohail T, Li Y. Alpha-lipoic acid improves the quality of ram spermatozoa stored at 4°C by reducing oxidative stress and increasing mitochondrial potential. Front Vet Sci. 2023;10:1345016. 10.3389/fvets.2023.1345016.
38. Jacoby AS, Busch-Nentwich E, Bryson-Richardson RJ, Hall TE, Berger J, Berger S, Sonntag C, Sachs C, Geisler R, Stemple DL, Currie PD. The zebrafish dystrophic mutant softy maintains muscle fibre viability despite basement membrane rupture and muscle detachment. Development. 2009;136(19):3367–76. 10.1242/dev.034561.
39. Matejas V, Hinkes B, Alkandari F, Al-Gazali L, Annexstad E, Aytac MB, Barrow M, Bláhová K, Bockenhauer D, Cheong HI, Maruniak-Chudek I, Cochat P, Dötsch J, Gajjar P, Hennekam RC, Janssen F, Kagan M, Kariminejad A, Kemper MJ, Koenig J, Kogan J, Kroes HY, Kuwertz-Bröking E, Lewanda AF, Medeira A, Muscheites J, Niaudet P, Pierson M, Saggar A, Seaver L, Suri M, Tsygin A, Wühl E, Zurowska A, Uebe S, Hildebrandt F, Antignac C, Zenker M. Mutations in the human laminin beta2 (LAMB2) gene and the associated phenotypic spectrum. Hum Mutat. 2010;31(9):992–1002. 10.1002/humu.21304.
40. Tzu J, Marinkovich MP. Bridging structure with function: structural, regulatory, and developmental role of laminins. Int J Biochem Cell Biol. 2008;40(2):199–214. 10.1016/j.biocel.2007.07.015.
41. Siu MK, Cheng CY. Extracellular matrix and its role in spermatogenesis. Adv Exp Med Biol. 2008;636:74–91. 10.1007/978-0-387-09597-4_5.
42. Pacheco RI, Cristo MI, Anjo SI, Silva AF, Sousa MI, Tavares RS, Sousa AP, Almeida Santos T, Moura-Ramos M, Caramelo F, Manadas B, Ramalho-Santos J, Amaral SG. New Insights on Sperm Function in Male Infertility of Unknown Origin: A Multimodal Approach. Biomolecules. 2023;13(10). 10.3390/biom13101462.

Figures

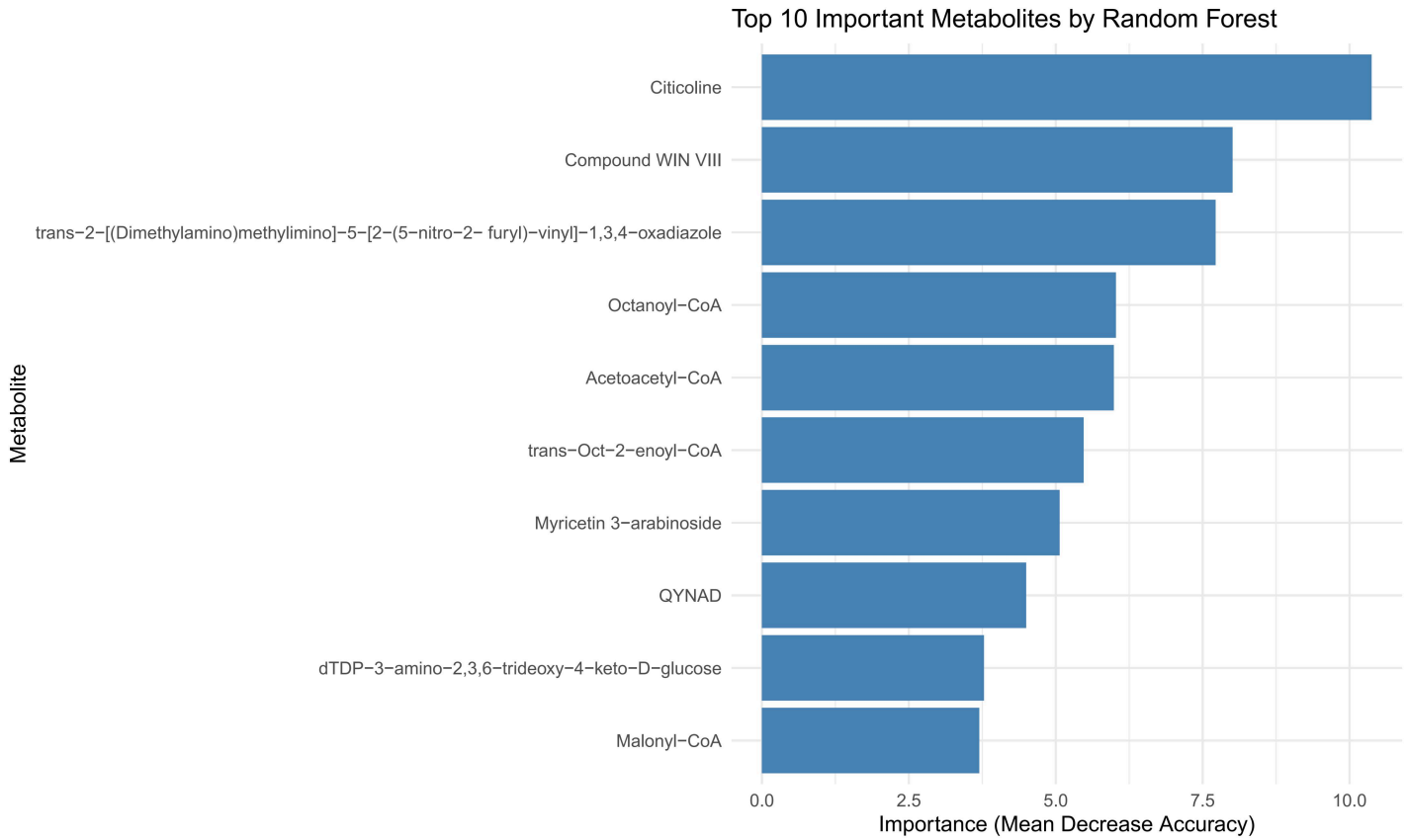


Figure 1

Screening of the top 10 metabolites based on the random forest (RF) model. Metabolites were ranked by importance scores calculated using mean decrease accuracy (MDA). The X-axis represents the importance value of each metabolite, and the Y-axis shows metabolite names.

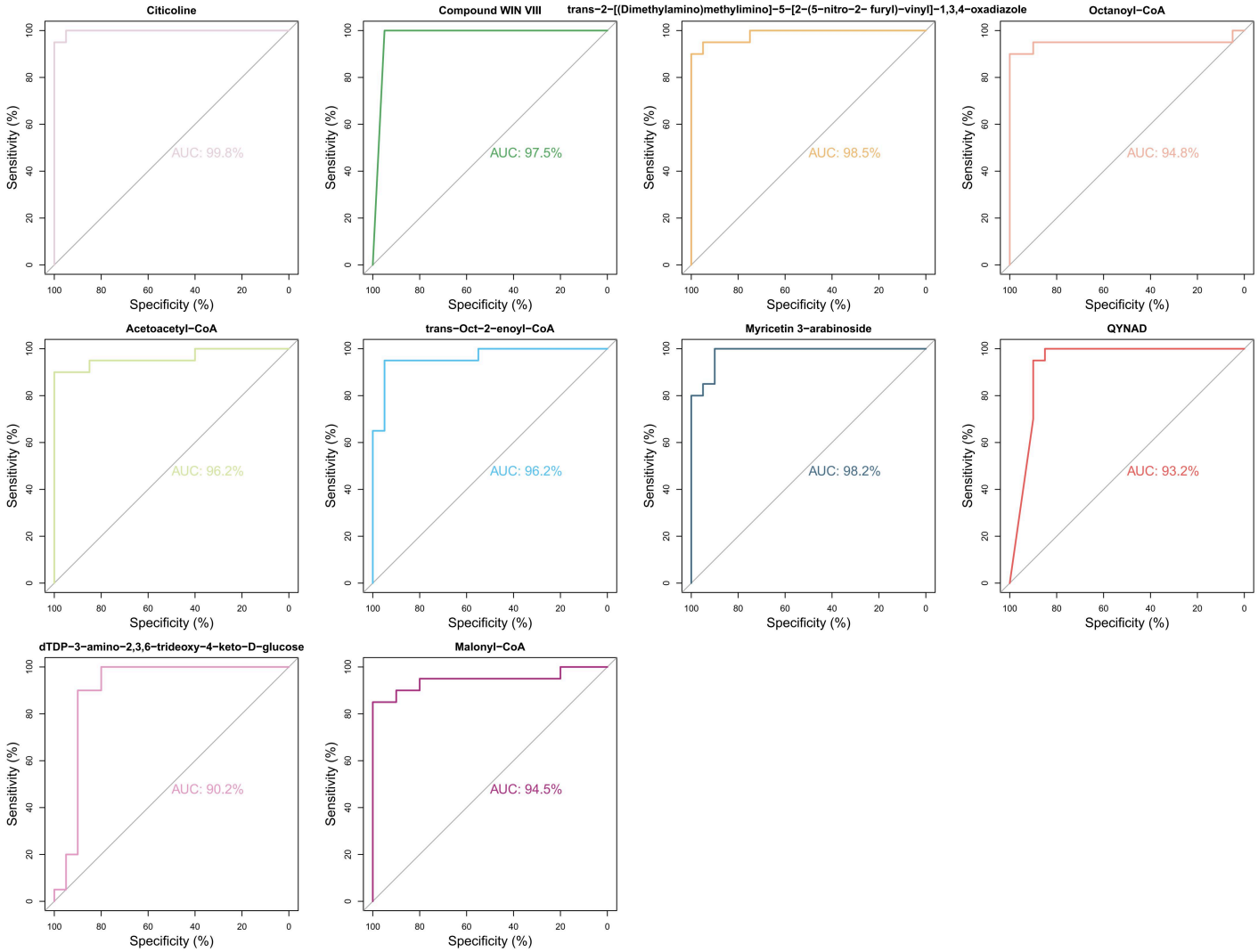


Figure 2

Receiver operating characteristic (ROC) curve analysis of the top 10 metabolites. The x-axis represents the specificity (%), and the y-axis represents the sensitivity (%).

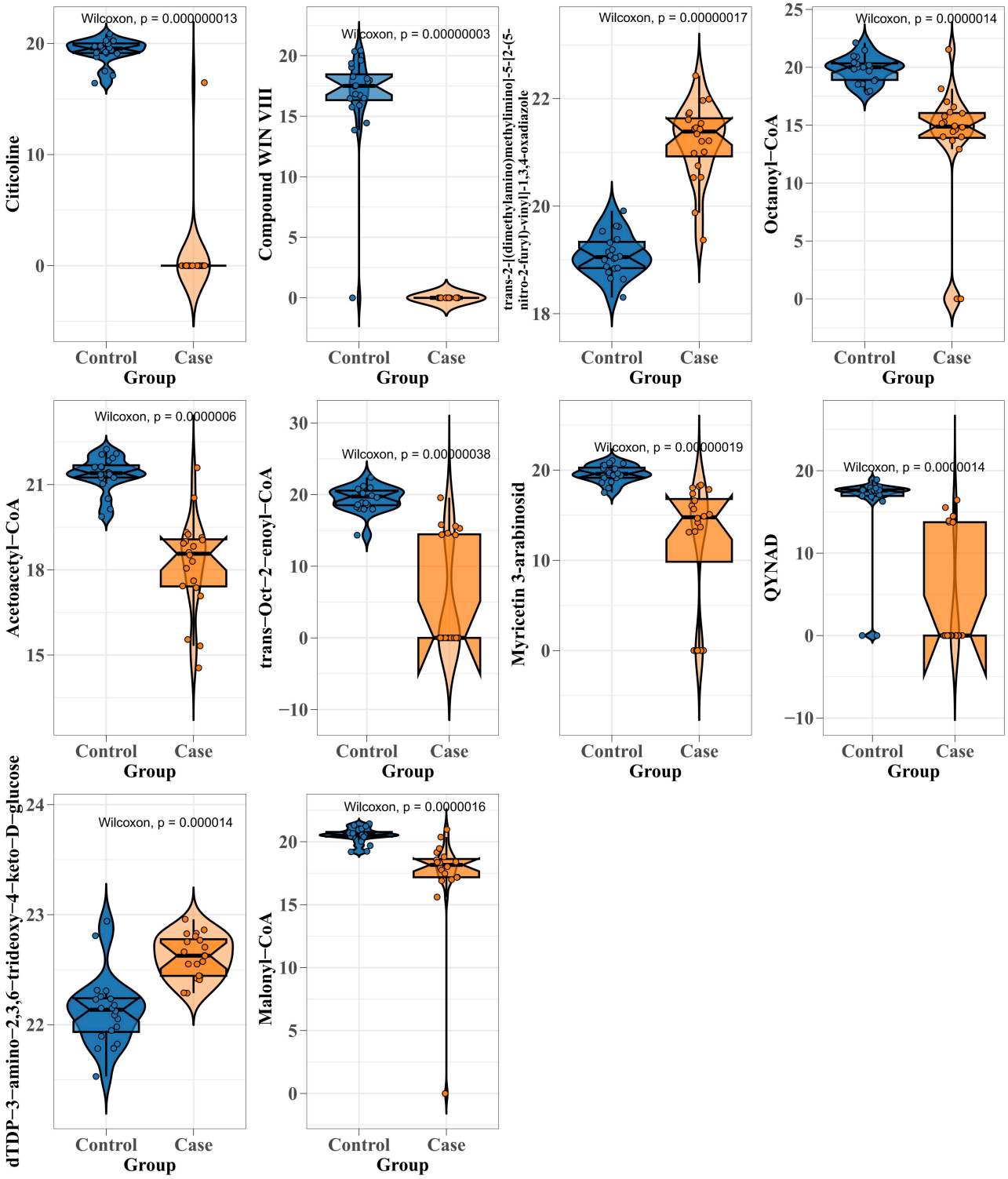


Figure 3

Abundance distribution of the top 10 metabolites. Each panel shows the distribution of metabolite levels in the control (blue) and azoospermia (orange) groups. Statistical comparisons were performed using the Wilcoxon rank-sum test, with the corresponding p-values indicated at the top of each plot.

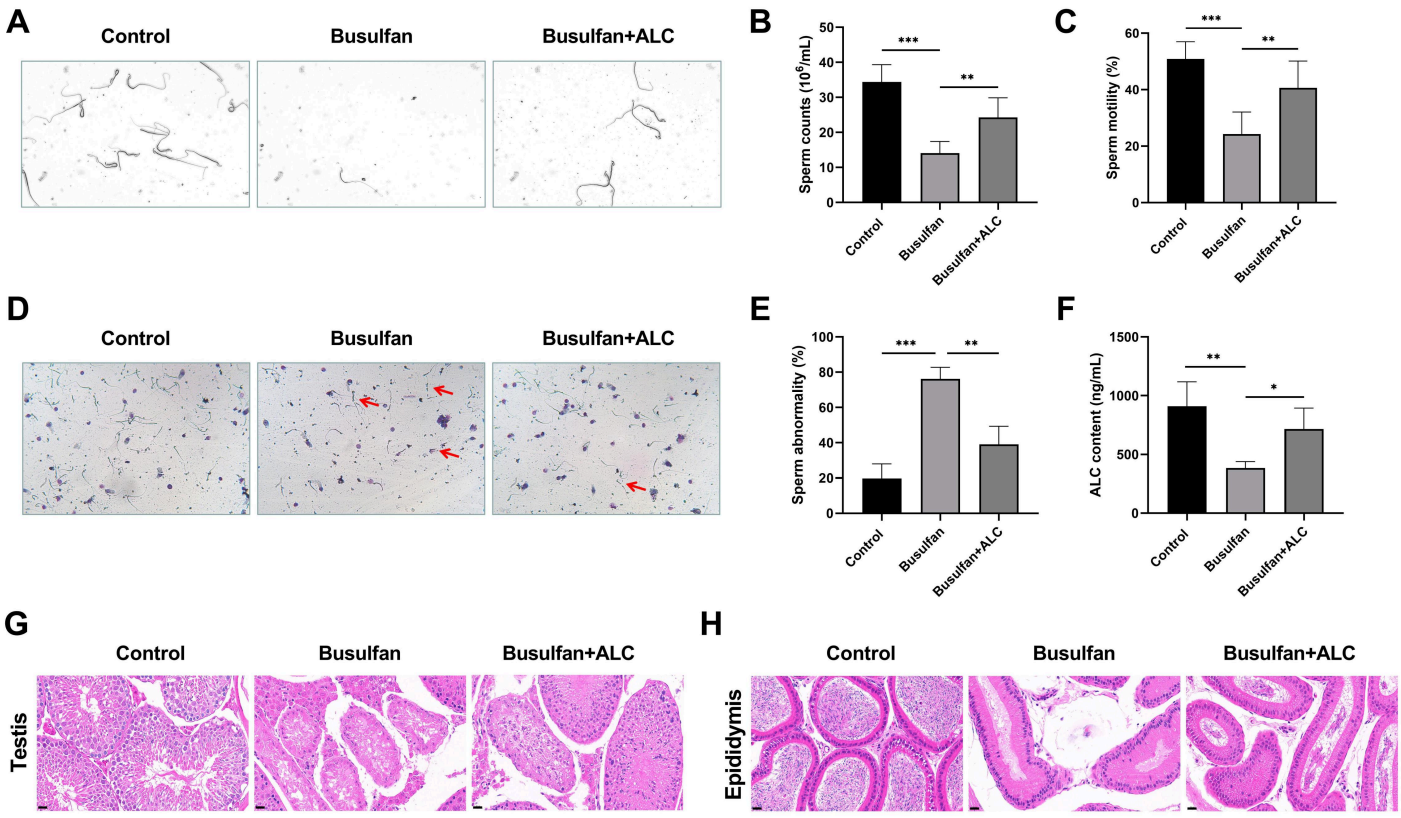


Figure 4

Acetyl L-carnitine (ALC) ameliorates busulfan-induced azoospermia in mice. (A) Microscopic observation of sperm morphology. Magnification: 400×. (B) Quantitative analysis of sperm concentration. (C) Assessment of sperm motility. (D) Giemsa staining of spermatozoa for morphological abnormality detection. Red arrows indicate morphologically abnormal spermatozoa. Magnification: 200×. (E) Sperm abnormality rate. (F) Determination of ALC content in testicular tissue. (G) Hematoxylin and eosin (HE) staining of testicular tissue. Scale bar: 20 μm; Magnification: 400×. (H) HE staining of epididymal tissue. Scale bar: 20 μm; Magnification: 400×. Data are presented as mean ± standard deviation (SD). * p-value < 0.05, ** p-value < 0.01, *** p-value < 0.001.

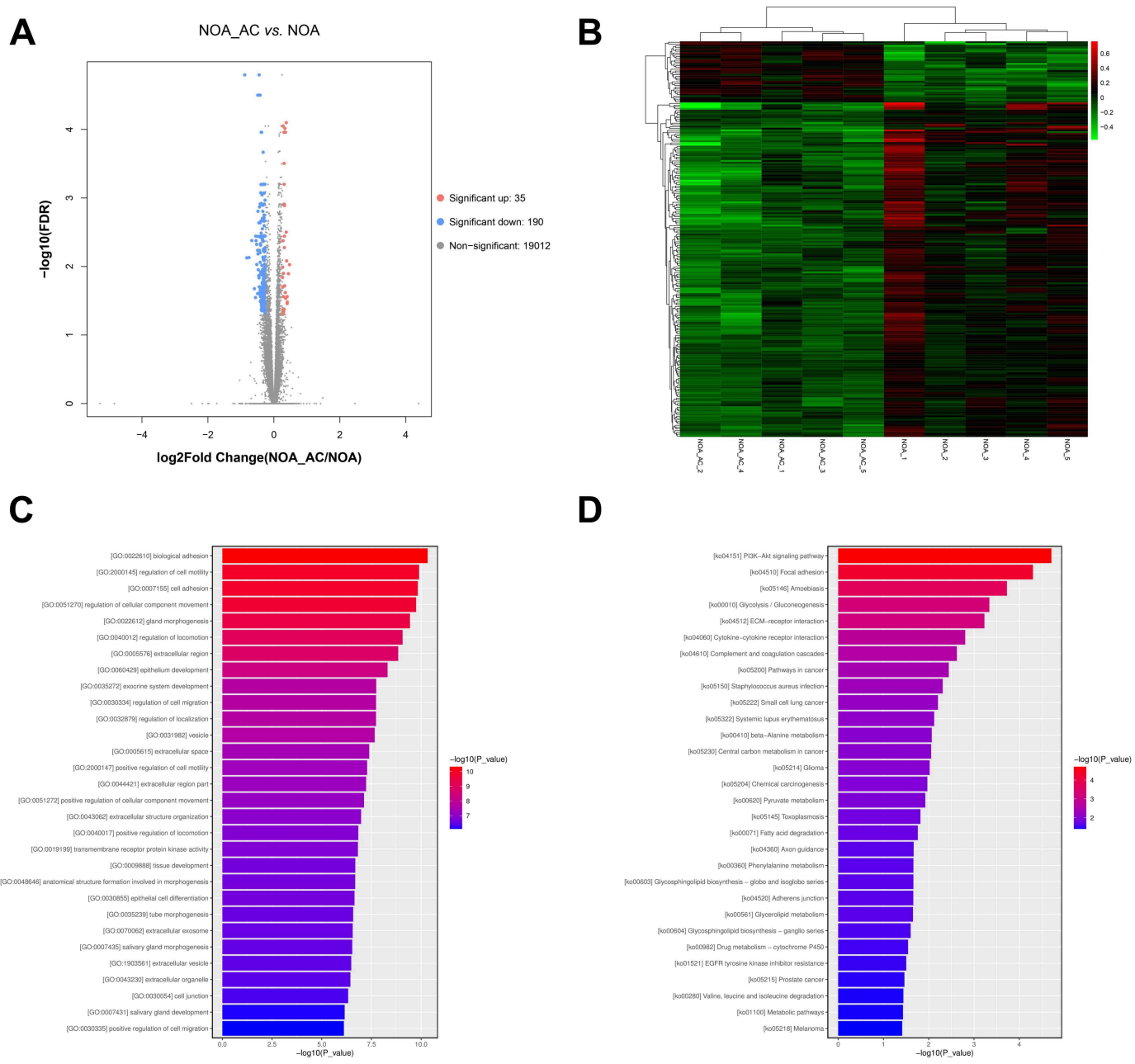


Figure 5

Transcriptomic differentially expressed genes (DEGs) profiling of ALC in busulfan-induced azoospermic mice. (A) Volcano plot of DEGs between the Busulfan and the Busulfan+ALC groups. Blue dots represent downregulated genes, red dots indicate upregulated genes, and gray dots denote genes with no significant differential expression. (B) Hierarchical clustering heatmap of DEGs. The color scale from green to red indicates low to high gene expression levels. (C) Gene Ontology (GO) enrichment analysis of DEGs. The bar plot displays the top enriched biological process, cellular component, and molecular function terms, with the x-axis representing the $\log_{10}$ (p-value). (D) Kyoto Encyclopedia of Genes and

Genomes (KEGG) pathway enrichment analysis of DEGs. The bar plot shows the significantly enriched signaling pathways, with the x-axis representing the p-value.

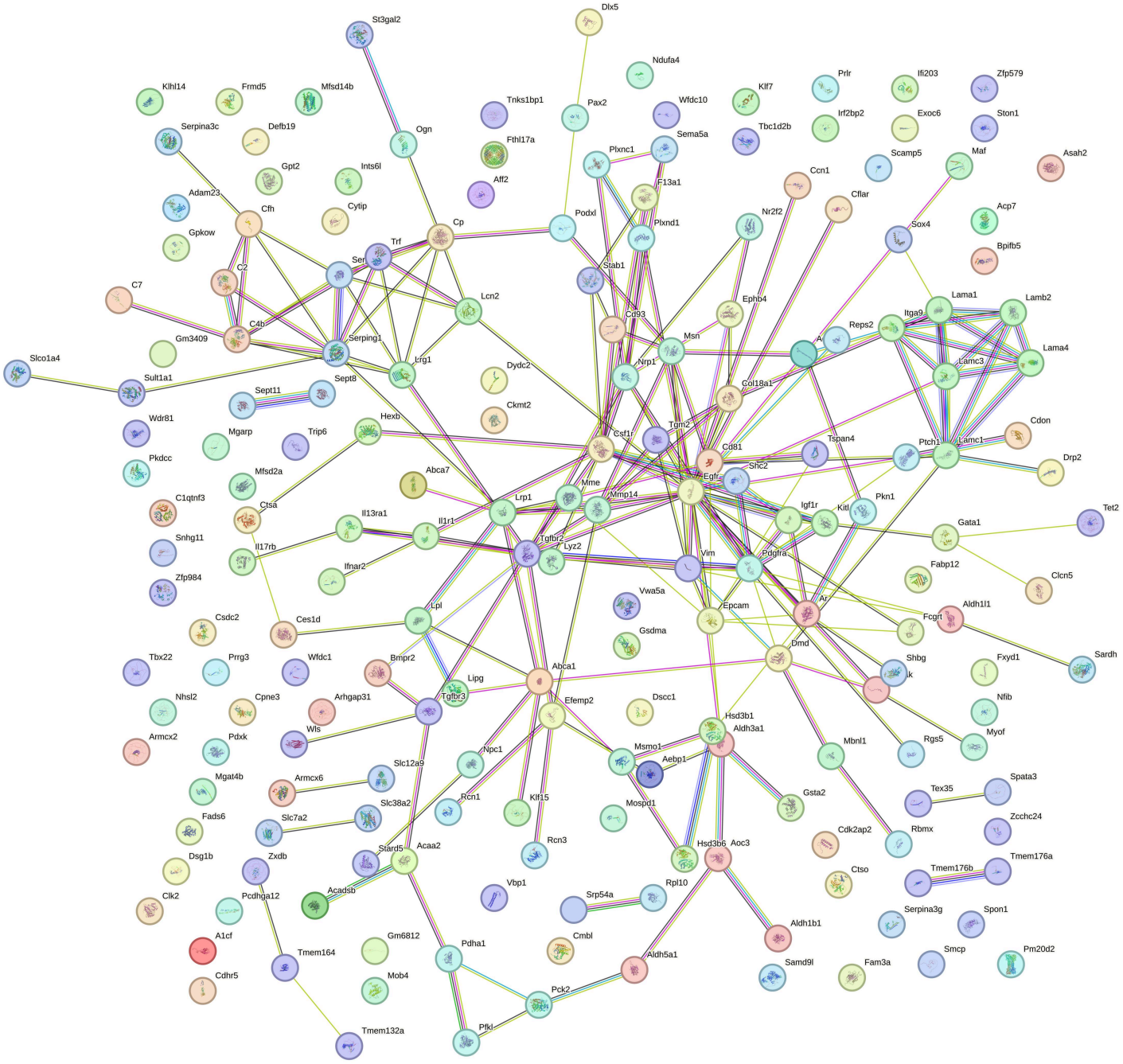


Figure 6

Protein-protein interaction (PPI) network of DEGs. Nodes represent genes, and edges indicate the interactions between genes.

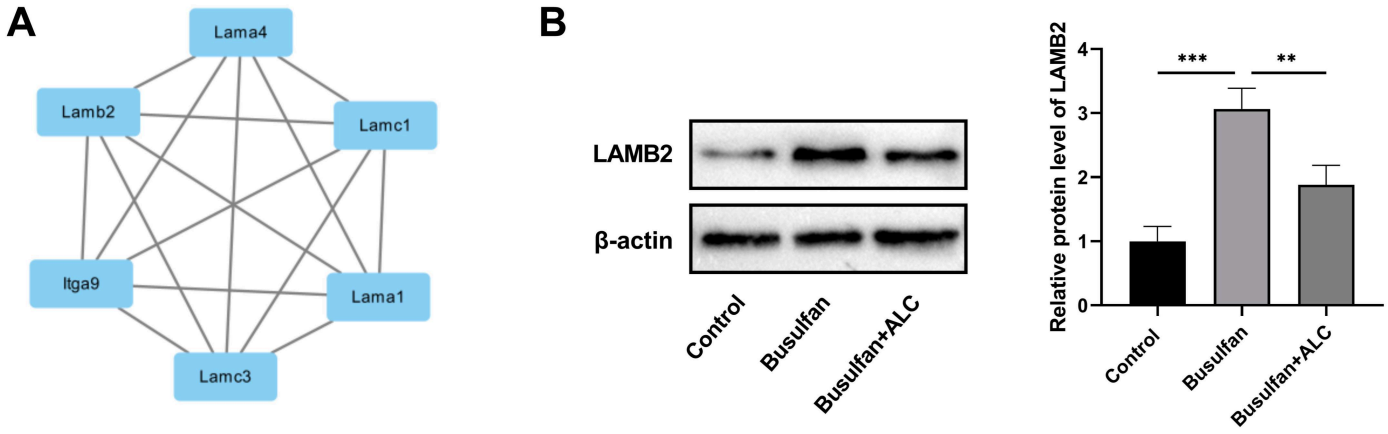


Figure 7

Identification of core genes and validation of laminin subunit beta 2 (LAMB2) protein expression. (A) Core gene identified. (B) The LAMB2 protein expression in testicular tissues. Data are presented as mean ± standard deviation (SD). ** p-value < 0.01, *** p-value < 0.001.

Supplementary Files

This is a list of supplementary files associated with this preprint. Click to download.

- SupplementaryFigure1.docx
- SupplementaryFigure2WB.pdf